# Axisymmetric motion of a generalized Rivlin-Ericksen fluids with shear-dependent normal stress coefficients

FERNANDO CARAPAU

*Abstract*—We analyze the unsteady flow of an incompressible generalized second-order fluid in a straight rigid tube, with circular cross-section of constant radius, where the normal stress coefficients depend on the shear rate by using a power law model. The full 3D unsteady model is simplified using a one-dimensional hierarchical approach based on the Cosserat theory related to fluid dynamics, which reduces the exact three-dimensional equations to a system depending only on time and on a single spatial variable. From this new system we obtain the relationship between mean pressure gradient and volume flow rate over a finite section of the tube. Attention is focused on some numerical simulation for unsteady/steady mean pressure gradient and on the analysis of perturbed flows.

*Keywords*—Cosserat theory, axisymmetric motion, mean pressure gradient, volume flow rate, perturbed flows, power law viscoelastic function.

## I. INTRODUCTION

Let us consider the Cauchy stress tensor for viscoelastic fluids of differential type (also called Rivlin-Ericksen fluids) with complexity $n = 2$, given by (see Colemann and Noll [11])

$$\boldsymbol{T} = -p\boldsymbol{I} + \mu\boldsymbol{A}_1 + \alpha_1\boldsymbol{A}_2 + \alpha_2\boldsymbol{A}_1^2 \qquad (1)$$

where $p$ is the pressure, $-p\boldsymbol{I}$ is the spherical part of the stress due to the constraint of incompressibility, $\mu$ is the coefficient of viscosity, and $\alpha_1$, $\alpha_2$ are material moduli

The author Fernando Carapau is with the Departamento de Matemática and CIMA-UE, Rua Romão Ramalho, Nº59, 7000-651, Évora-Portugal (e-mail: flc@uevora.pt).

which are usually referred to as the normal stress coefficients. The kinematical first two Rivlin-Ericksen tensors $\boldsymbol{A}_1$ and $\boldsymbol{A}_2$ are defined through (see Rivlin and Ericksen [12])

$$\boldsymbol{A}_1 = \nabla\boldsymbol{\vartheta} + \left(\nabla\boldsymbol{\vartheta}\right)^T \qquad (2)$$

and

$$\boldsymbol{A}_2 = \frac{d}{dt}\boldsymbol{A}_1 + \boldsymbol{A}_1\nabla\boldsymbol{\vartheta} + \left(\nabla\boldsymbol{\vartheta}\right)^T\boldsymbol{A}_1 \qquad (3)$$

where $\boldsymbol{\vartheta}$ is the velocity of the fluid and $\frac{d}{dt}(\cdot)$ denotes the material time derivative. In equation (3) the material time derivative of the tensor $\boldsymbol{A}_1$ is given by

$$\frac{d}{dt}\boldsymbol{A}_1 = \frac{\partial}{\partial t}\boldsymbol{A}_1 + \boldsymbol{\vartheta} \cdot \nabla\boldsymbol{A}_1.$$

The classical constitutive equation related with Newtonian fluids is recovered with $\alpha_1 = \alpha_2 = 0$ at equation (1). The thermodynamics and stability of the fluids related with the Cauchy stress tensor (1) have been studied in detail by Dunn and Fosdick (see [13]) who showed that if the fluid is to be compatible with thermodynamics in the sense that all motions of the fluid meet the Clausius-Duhem inequality and the assumption that the specific Helmholtz free energy of the fluid is a minimum in equilibrium, then

$$\mu \geqslant 0, \quad \alpha_1 \geqslant 0, \quad \alpha_1 + \alpha_2 = 0. \qquad (4)$$

Fosdick and Rajagopal (see [14]), based on the experimental observation, showed that for many non-Newtonian fluids of current rheological interest the reported values for $\alpha_1$ and $\alpha_2$ do not satisfy the restriction $(4)_{2,3}$, relaxed that assumption. Also, they showed that for arbitrary values of $\alpha_1 + \alpha_2$, with $\alpha_1 < 0$, a fluid filling a compact domain and adhering to the boundary of the domain exhibits an anomalous behavior not expected on real fluids. The condition $(4)_3$ simplifies substantially the mathematical model and the corresponding analysis. The fluids characterized by (4) are known as second-grade fluids as opposed to the general second-order fluids. The terminology "grade" is used in the place of "order" to convey the notion of "exactness" rather than the

notion of "approximation" wherein the model is not required to be compatible with thermodynamics. It should also be added that the use of Clausius-Duheim inequality is the subject matter of much controversy (see e.g. Coscia and Galdi [15]). Experimental studies with polymers (see e.g. Beracea et al. [3]), suspensions (see e.g. Mall-Gleissle et al. [2]) and liquid crytals (see e.g. Tao et al. [16]) seem to indicate that for several fluids, one does observe a substancial variation in normal stress effects with the shear rate. In fact, Harris (see [1]) even argues that this dependence for specific flow regimes is of a power law nature. Therefore, we consider an extension of the Rivlin-Ericksen fluid model of second-order by introducing a shear-dependent function of power law related with the normal stress coefficients. With this in mind, the constitutive equation (1), becomes

$$\boldsymbol{T} = -p\boldsymbol{I} + \mu\boldsymbol{A}_1 + \alpha(|\dot{\gamma}|)(\alpha_1\boldsymbol{A}_2 + \alpha_2\boldsymbol{A}_1^2) \qquad (5)$$

where

$$\alpha(|\dot{\gamma}|) : \mathbb{R}^+ \to \mathbb{R}^+$$

is the shear-dependent normal stress coefficients function and $\dot{\gamma}$ is a scalar measure of the rate of shear defined by $|\dot{\gamma}| = \sqrt{2\boldsymbol{D} : \boldsymbol{D}}$ with

$$\boldsymbol{D} := \frac{1}{2}\big(\nabla\boldsymbol{\vartheta} + (\nabla\boldsymbol{\vartheta})^T\big)$$

being the rate of deformation tensor. The particular functional dependence of the normal stress coefficients on shear rate is generally chosen in order to fit experimental data and, in the case of a power law fluid model, is given by

$$\alpha(|\dot{\gamma}|) = k|\dot{\gamma}|^{n-1} \qquad (6)$$

where the parameters $k$ and $n$ are positive constants called the consistency and the flow index related with the normal stress coefficients. If $n = 1$ in (6), the Cauchy stress tensor (5) corresponds to the constitutive equation (1) with $k = 1$. If $n < 1$ at (6) then

$$\lim_{|\dot{\gamma}| \to +\infty} \alpha(|\dot{\gamma}|) = 0, \quad \lim_{|\dot{\gamma}| \to 0} \alpha(|\dot{\gamma}|) = +\infty,$$

and we have a shear-thinning fluid behaviour (viscoelastic decreases monotonically with shear rate). For $n > 1$ at (6), we get

$$\lim_{|\dot{\gamma}| \to +\infty} \alpha(|\dot{\gamma}|) = +\infty, \quad \lim_{|\dot{\gamma}| \to 0} \alpha(|\dot{\gamma}|) = 0,$$

and the fluid shows a shear-thickening behaviour (viscoelastic increases with shear rate). This theoretical

model has limited applications to real fluids due to the unboundedness of the viscoelastic function, but is widely used and can be accurate for specific flow regimes. The theoretical study of the model associated to the constitutive equation (5), namely existence, uniqueness and regularity of classical and weak solutions with any $\alpha_1, \alpha_2 \in \mathbb{R}$ still poses some difficulties. In this paper we are interested in the numerical study of the model associated to equation (5) with condition (6), using for that the director approach (also called Cosserat Theory) related to fluid dynamics, developed by Caulk and Naghdi [4]. The relevance of using this theory is not in regarding it as an approximation to three-dimensional equations, but rather in their use as independent theories to predict some of the main properties of the three-dimensional problems. Advantages of the director theory include: (i) the theory incorporates all components of the linear momentum; (ii) it is a hierarchical theory, making it possible to increase the accuracy of the model; (iii) the flow is not assumed to be uni-directional; (iv) it is unnecessary to make assumptions about the form of the nonlinear and (v) the wall shear stress enters directly in the formulation as a dependent variable.

Recently, this theory approach has been applied to haemodynamics by Robertson et al. [5] and Carapau et al. [6]. Also by Carapau and Sequeira [7], [8], [9], and by Carapau [10] considering non-Newtonian fluids. This theory it was validated on the special case of a uniform tube of constant radius for Newtonian fluid (see [4]), and also for non-Newtonian fluids (see [6], [7]). Using the director theory (see [4]) the velocity field[1] $\boldsymbol{\vartheta} = \boldsymbol{\vartheta}(x_1, x_2, z, t)$, can be approximated by the following finite series[2]:

$$\boldsymbol{\vartheta} = \boldsymbol{v} + \sum_{N=1}^{k} x_{\alpha_1} \dots x_{\alpha_N} \boldsymbol{W}_{\alpha_1\dots\alpha_N}, \qquad (7)$$

with

$$\boldsymbol{v} = v_i(z, t)\boldsymbol{e}_i, \quad \boldsymbol{W}_{\alpha_1\dots\alpha_N} = W_{\alpha_1\dots\alpha_N}^i(z, t)\boldsymbol{e}_i. \qquad (8)$$

Here, $\boldsymbol{v}$ represents the velocity along the axis of symmetry $z$ at time $t$, $x_{\alpha_1} \dots x_{\alpha_N}$ are polynomial weighting functions with order $k$ (the number $k$ identifies the order of the hierarchical theory and is related to the number of

---

[1]Here, we consider $x_i (i = 1, 2, 3)$ the rectangular cartesian coordenates and for convenience set $x_3 = z$.

[2]Latin indices subscript take the values $1, 2, 3$, Greek indices subscript $1, 2$. Summation convention is employed over a repeated index.

directors), the vectors $\boldsymbol{W}_{\alpha_1\dots\alpha_N}$ are the director velocities which are completely symmetric with respect to their indices and $\boldsymbol{e}_i$ are the associated unit basis vectors. From this velocity field approach that we use to predict some of the main properties of the three-dimensional problem, we obtain the axisymmetric unsteady relationship between mean pressure gradient and volume flow rate over a finite section of a straight tube with circular cross-section and constant radius.

## II. GOVERNING EQUATIONS

Let us consider the axisymmetric motion, about the $z$ axis, of an incompressible fluid, without body forces, inside a straight and impermeable tube $\Omega$ with circular cross-section contained in $\mathbb{R}^3$ (see Figure 1). Also, let us consider the surface scalar function $\phi(z,t)$, that is related with the cross-section of the tube by the following relationship

$$\phi^2(z,t) = x_1^2 + x_2^2. \tag{9}$$

The boundary $\partial\Omega$ is composed by $\Gamma_1$ (proximal cross-section), $\Gamma_2$ (distal cross-section) and by $\Gamma_w$ the lateral wall of the tube. The equations of motion, stating the
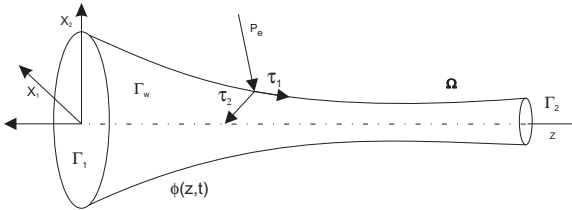


Fig. 1: Fluid domain $\Omega$ with the tangential components of the surface traction vector $\tau_1, \tau_2$ and $p_e$, where $\phi(z,t)$ denote the radius of the domain surface along the axis of symmetry $z$ at time $t$.

conservation of linear momentum and mass are given in $\Omega \times (0,T)$ by

$$\begin{cases} \rho\Big(\dfrac{\partial\boldsymbol{\vartheta}}{\partial t} + \boldsymbol{\vartheta}\cdot\nabla\boldsymbol{\vartheta}\Big) = \nabla\cdot\boldsymbol{T}, \\[2ex] \nabla\cdot\boldsymbol{\vartheta} = 0, \\[2ex] \boldsymbol{T} = -p\boldsymbol{I} + \boldsymbol{\sigma}, \ \ \boldsymbol{t}_W = \boldsymbol{T}\cdot\boldsymbol{\eta}, \end{cases} \tag{10}$$

with the initial condition

$$\boldsymbol{\vartheta}(x,0) = \boldsymbol{\vartheta}_0(x) \ \text{ in } \ \Omega, \tag{11}$$

and the homogeneous Dirichlet boundary condition

$$\boldsymbol{\vartheta}(x,t) = 0 \ \text{ on } \ \Gamma_w \times (0,T), \tag{12}$$

where $\boldsymbol{\vartheta} = \vartheta_i\boldsymbol{e}_i$ is the velocity field and $\rho$ is the constant fluid density. Equation $(10)_1$ represents the balance of linear momentum and $(10)_2$ is the incompressibility condition. In equation $(10)_3$, $\boldsymbol{t}_W$ denotes the stress vector on a surface whose outward unit normal is $\boldsymbol{\eta} = \eta_i\boldsymbol{e}_i$, and $\boldsymbol{\sigma}$ is the extra stress tensor given by

$$\boldsymbol{\sigma} = \mu\boldsymbol{A}_1 + \alpha\big(|\dot{\gamma}|\big)\big(\alpha_1\boldsymbol{A}_2 + \alpha_2\boldsymbol{A}_1^2\big) \tag{13}$$

where the shear-dependent normal stress coefficients is giving by (6). The kinematical first two Rivlin-Ericksen tensors $\boldsymbol{A}_1$ and $\boldsymbol{A}_2$ are given by (2) and (3), respectively. The components of the outward unit normal to the surface $\phi(z,t)$ are

$$\eta_1 = \frac{x_1}{\phi\sqrt{1+\phi_z^2}}, \ \eta_2 = \frac{x_2}{\phi\sqrt{1+\phi_z^2}}, \ \eta_3 = -\frac{\phi_z}{\sqrt{1+\phi_z^2}}, \tag{14}$$

where the subscript variable denotes partial differentiation. Since equation (9) defines a material surface, the velocity field $\boldsymbol{\vartheta}$ must satisfy the kinematic condition

$$\frac{d}{dt}\big(\phi^2(z,t) - x_1^2 - x_2^2\big) = 0,$$

i.e.

$$\phi\phi_t + \phi\phi_z\vartheta_3 - x_1\vartheta_1 - x_2\vartheta_2 = 0 \tag{15}$$

on the boundary (9). Averaged quantities such as flow rate and average pressure are needed to study 1D models. Consider $S(z,t)$ as a generic axial section of the tube at time $t$ defined by the spatial variable $z$ and bounded by the circle defined in (9) and let $A(z,t)$ be the area of this section $S(z,t)$. Then, the volume flow rate $Q$ is defined by

$$Q(z,t) = \int_{S(z,t)} \vartheta_3(x_1,x_2,z,t)dx, \tag{16}$$

and the average pressure $\bar{p}$, by

$$\bar{p}(z,t) = \frac{1}{A(z,t)} \int_{S(z,t)} p(x_1,x_2,z,t)dx. \tag{17}$$

Now, starting with representation (7), with $k = 3$, it follows (see [4]) that the approximation of the velocity field $\boldsymbol{\vartheta} = \vartheta_i(x_1,x_2,z,t)\boldsymbol{e}_i$ using nine directors, is given by

$$\begin{aligned} \boldsymbol{\vartheta} &= \Big[x_1(\xi + \lambda(x_1^2 + x_2^2))\Big]\boldsymbol{e}_1 \\ &+ \Big[x_2(\xi + \lambda(x_1^2 + x_2^2))\Big]\boldsymbol{e}_2 \\ &+ \Big[v_3 + \theta(x_1^2 + x_2^2)\Big]\boldsymbol{e}_3 \end{aligned} \tag{18}$$

3

where $\xi, \theta, \lambda$ are scalar functions of the spatial variable $z$ and time $t$. The physical significance of these scalar functions in (18) is the following: $\theta$ is related to transverse shearing motion, while $\xi$ and $\lambda$ are related to transverse elongation.

Let us consider a flow in a rigid tube, i.e.

$$\phi = \phi(z), \tag{19}$$

From (19), (16), (18), (10)$_2$ and (12) the volume flow rate $Q$ is just a function of time $t$, given by

$$Q(t) = \frac{\pi}{2}\,\phi^2(z)v_3(z,t). \tag{20}$$

Then, for a flow in a rigid tube, with volume flow rate (20) and conditions (12) and (10)$_2$, the velocity field (18) becomes (see [4])

$$\begin{aligned}
\boldsymbol{\vartheta} &= \left[x_1\left(1 - \frac{x_1^2 + x_2^2}{\phi^2}\right)\frac{2\phi_z Q(t)}{\pi\phi^3}\right]\boldsymbol{e}_1 \\
&+ \left[x_2\left(1 - \frac{x_1^2 + x_2^2}{\phi^2}\right)\frac{2\phi_z Q(t)}{\pi\phi^3}\right]\boldsymbol{e}_2 \\
&+ \left[\frac{2Q(t)}{\pi\phi^2}\left(1 - \frac{x_1^2 + x_2^2}{\phi^2}\right)\right]\boldsymbol{e}_3.
\end{aligned} \tag{21}$$

The stress vector on the lateral surface $\Gamma_w$ (see [4]) in terms of the outward unit normal and tangential components $\tau_1, \tau_2$ and $p_e$ (see Figure 1) is given by

$$\begin{aligned}
\boldsymbol{t}_W &= \left[\frac{1}{\phi\sqrt{1+\phi_z^2}}\Big(\tau_1 x_1\phi_z - p_e x_1 - \tau_2 x_2(1+\phi_z^2)^{1/2}\Big)\right]\boldsymbol{e}_1 \\
&+ \left[\frac{1}{\phi\sqrt{1+\phi_z^2}}\Big(\tau_1 x_2\phi_z - p_e x_2 + \tau_2 x_1(1+\phi_z^2)^{1/2}\Big)\right]\boldsymbol{e}_2 \\
&+ \left[\frac{1}{\sqrt{1+\phi_z^2}}\Big(\tau_1 + p_e\phi_z\Big)\right]\boldsymbol{e}_3.
\end{aligned} \tag{22}$$

Instead of satisfying the momentum equation (10)$_1$ pointwise in the fluid, we impose the following integral conditions:

$$\int_{S(z,t)}\left[\nabla\cdot\boldsymbol{T} - \rho\left(\frac{\partial\boldsymbol{\vartheta}}{\partial t} + \boldsymbol{\vartheta}\cdot\nabla\boldsymbol{\vartheta}\right)\right]dx = 0, \tag{23}$$

$$\int_{S(z,t)}\left[\nabla\cdot\boldsymbol{T} - \rho\left(\frac{\partial\boldsymbol{\vartheta}}{\partial t} + \boldsymbol{\vartheta}\cdot\nabla\boldsymbol{\vartheta}\right)\right]x_{\alpha_1}\ldots x_{\alpha_N}dx = 0, \tag{24}$$

where $N = 1, 2, 3$.

Using the divergence theorem and integration by parts, equations $(23) - (24)$ can be reduced to the four vector equations:

$$\frac{\partial\boldsymbol{n}}{\partial z} + \boldsymbol{f} = \boldsymbol{a}, \tag{25}$$

$$\frac{\partial\boldsymbol{m}^{\alpha_1\ldots\alpha_N}}{\partial z} + \boldsymbol{l}^{\alpha_1\ldots\alpha_N} = \boldsymbol{k}^{\alpha_1\ldots\alpha_N} + \boldsymbol{b}^{\alpha_1\ldots\alpha_N}, \tag{26}$$

where $\boldsymbol{n}$, $\boldsymbol{k}^{\alpha_1\ldots\alpha_N}$, $\boldsymbol{m}^{\alpha_1\ldots\alpha_N}$ are resultant forces defined by

$$\boldsymbol{n} = \int_S \boldsymbol{T}_3 dx, \quad \boldsymbol{k}^\alpha = \int_S \boldsymbol{T}_\alpha dx, \tag{27}$$

$$\boldsymbol{k}^{\alpha\beta} = \int_S \left(\boldsymbol{T}_\alpha x_\beta + \boldsymbol{T}_\beta x_\alpha\right)dx, \tag{28}$$

$$\boldsymbol{k}^{\alpha\beta\gamma} = \int_S \left(\boldsymbol{T}_\alpha x_\beta x_\gamma + \boldsymbol{T}_\beta x_\alpha x_\gamma + \boldsymbol{T}_\gamma x_\alpha x_\beta\right)dx, \tag{29}$$

$$\boldsymbol{m}^{\alpha_1\ldots\alpha_N} = \int_S \boldsymbol{T}_3 x_{\alpha_1}\ldots x_{\alpha_N}dx. \tag{30}$$

The quantities $\boldsymbol{a}$ and $\boldsymbol{b}^{\alpha_1\ldots\alpha_N}$ are inertia terms defined by

$$\boldsymbol{a} = \int_S \rho\left(\frac{\partial\boldsymbol{\vartheta}}{\partial t} + \boldsymbol{\vartheta}\cdot\nabla\boldsymbol{\vartheta}\right)dx, \tag{31}$$

$$\boldsymbol{b}^{\alpha_1\ldots\alpha_N} = \int_S \rho\left(\frac{\partial\boldsymbol{\vartheta}}{\partial t} + \boldsymbol{\vartheta}\cdot\nabla\boldsymbol{\vartheta}\right)x_{\alpha_1}\ldots x_{\alpha_N}dx, \tag{32}$$

and $\boldsymbol{f}$, $\boldsymbol{l}^{\alpha_1\ldots\alpha_N}$, which arise due to surface traction on the lateral boundary, are defined by

$$\boldsymbol{f} = \int_{\partial S} \sqrt{1+\phi_z^2}\,\boldsymbol{t}_W dx, \tag{33}$$

$$\boldsymbol{l}^{\alpha_1\ldots\alpha_N} = \int_{\partial S} \sqrt{1+\phi_z^2}\,\boldsymbol{t}_W\,x_{\alpha_1}\ldots x_{\alpha_N}dx. \tag{34}$$

The equation for the mean pressure gradient as a function of the volume flow rate will be obtained using the results quantities $(27) - (34)$ on equations $(25) - (26)$.

## III. SOME NUMERICAL RESULTS

Let us consider the system $(10) - (13)$ where the normal stress coefficients $\alpha_1$ and $\alpha_2$ do not satisfy the restriction $(4)_{2,3}$. We consider the case of a straight circular rigid tube with constant radius, i.e. $\phi = cts$. Now, taking into account the velocity approach (21), we obtain the quantities $(27) - (34)$. Using that quantities on equations $(25) - (26)$, we get the following unsteady relationship

$$\begin{aligned}
\bar{p}_z(z,t) &= -\frac{8\mu}{\pi\phi^4}Q(t) - \frac{4\rho}{3\pi\phi^2}\Big[1 + \tag{35} \\
&+ \frac{3k\alpha_1}{4\rho}\frac{2^{\frac{5n+5}{2}}}{(n+3)\pi^{n-1}\phi^{3n-1}}Q^{n-1}(t)\Big]\dot{Q}(t),
\end{aligned}$$

where the notation $\dot{Q}(t)$ is used for time differentiation. Integrating equation (35), over a finite section of the tube

(with $z_1 < z_2$), we obtain the mean pressure gradient $G(t)$ as a function of the volume flow rate:

$$G(t) = \frac{8\mu}{\pi\phi^4}Q(t) + \frac{4\rho}{3\pi\phi^2}\Big[1 + \tag{36}$$

$$+ \frac{3k\alpha_1}{4\rho}\frac{2^{\frac{5n+5}{2}}}{(n+3)\pi^{n-1}\phi^{3n-1}}Q^{n-1}(t)\Big]\dot{Q}(t),$$

where

$$G(t) = \frac{\bar{p}(z_1,t) - \bar{p}(z_2,t)}{z_2 - z_1}.$$

Setting $\alpha_1 = 0$ in (36), we recover the solution for Newtonian viscous fluid obtain by Caulk and Naghdi (see [4]). Also, considering $n = k = 1$ in (36), we recover the solution for second-order viscoelastic fluid obtain by Carapau and Sequeira (see [7]). Now, let us consider the following dimensionless variables

$$\hat{t} = \omega_0 t, \ \ \hat{Q} = \frac{2\rho}{\pi\phi\mu}Q, \ \ \hat{G} = \frac{\rho\phi^3}{\mu^2}G \tag{37}$$

where $\phi$ is the characteristic radius of the tube and $\omega_0$ is the characteristic frequency for unsteady flows. In the case where a steady flow rate is specified, the nondimensional flow rate $\hat{Q}$ is identical to the classical Reynolds number (see e.g. [5]). Now, substituting the dimensionless variables (37) into equation (36), we obtain

$$\hat{G}(\hat{t}) = 4\hat{Q}(\hat{t}) + \frac{2}{3}\Big[1 + 3\mathcal{W}_e\frac{2^{\frac{3n+3}{2}}}{n+3}\hat{Q}^{n-1}(\hat{t})\Big]\mathcal{W}_0^2\,\dot{\hat{Q}}(\hat{t}) \tag{38}$$

where $\mathcal{W}_0 = \phi\sqrt{\rho\omega_0/\mu}$ is the Womersley number and

$$\mathcal{W}_e = \frac{|\alpha_1|k^{n-1}}{\phi^{2n}\rho^n}$$

is a viscoelastic parameter, also called the Weissenberg number (see e.g. Galdi et al. [17]). The dimensionless number $\mathcal{W}_0$ is the most commonly used parameter to reflect the pulsatility of the flow, which is an unsteady phenomenon. Solving equation (38), we can compute the volume flow rate $\hat{Q}(\hat{t})$ in terms of the mean pressure gradient $\hat{G}(\hat{t})$ for different values of the Womersley number, Weissenberg number and flow index $n$. Also, we can give some considerations about perturbed flows.

### Flow under constant mean pressure gradient

Considering a constant mean pressure gradient $\hat{G}(\hat{t}) = \hat{G}_0$ the system converges toward a steady state solution. In Figure 2 this steady state volume flow rate is obtained solving the time dependent problem but, if we
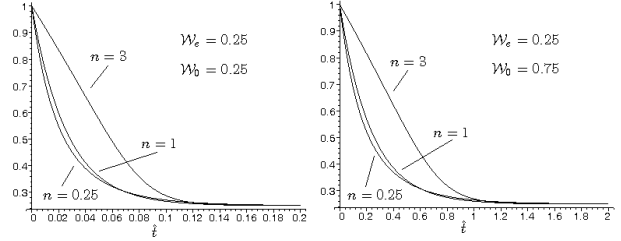


Fig. 2: Time evolution of the volume flow rate (38), with fixed Weissenberg number ($\mathcal{W}_e = 0.25$), for different values of the Womersley number ($\mathcal{W}_0 = (0.25, 0.75)$) and different values of the flow index ($n = (0.25, 1, 3)$). Here we consider $\hat{G}_0 = 1$.

are not interested in the behavior during the initial transient phase, the steady (asymptotic) value of the volume flow rate can be obtained directly from (38) setting

$$\dot{\hat{Q}}(\hat{t}) = 0,$$

since at constant pressure gradient, $\dot{\hat{Q}}(t)$ converges to zero as $\hat{t}$ goes to infinity, i.e.

$$\lim_{\hat{t}\to+\infty}\dot{\hat{Q}}(\hat{t}) = 0.$$

Therefore the nondimensional steady solution is characterized by

$$\hat{Q} = \hat{G}_0/4, \tag{39}$$

which is in excellent agreement with the numerical results illustrated in Figure 2. There is a linear relation between quantities $\hat{Q}$ and $\hat{G}_0$ in (39). From Figure 2, we can realize that there is no qualitative difference between solutions for different values of flow index. Considering other values for Womersley and Weissenberg numbers we get the same solution behavior shown in Figure 2.

### Flow under time dependent mean pressure gradient

Now, we consider the general situation of imposing a time dependent mean pressure gradient on relation (38). We will only briefly show same numerical results for specific mean pressure gradient. Considering the following mean pressure gradient

$$\hat{G}(\hat{t}) = 1 + |sin(\hat{t})| + |cos(2\hat{t})|, \tag{40}$$

we can observe in Figure 3 how the volume flow rate $\hat{Q}$ change with the time for different values of flow index, Womersley and Weissenberg numbers. From these results we can realize that there is no qualitative different

between solutions, after initial transient phase, for fixed Womersley number. However, the behavior of the sinusoidal solution start to decrease the values on the peacks when we increase the flow index and the Weissenberg number.
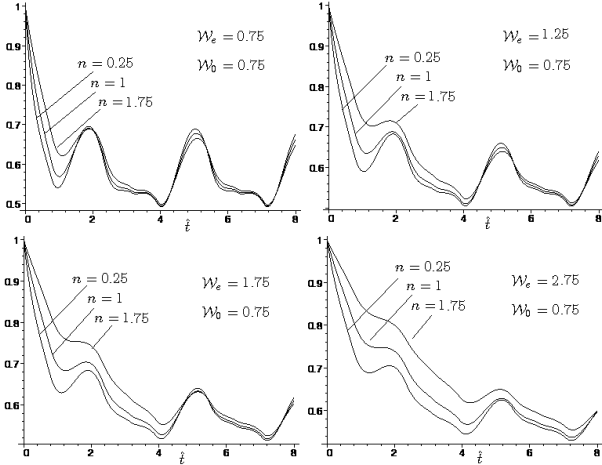


Fig. 3: Time evolution of the volume flow rate given by (38) with mean pressure gradient (40), with fixed Womersley number ($\mathcal{W}_0 = 0.75$), for different values of the Weissenberg number ($\mathcal{W}_e = (0.75, 1.25, 1.75, 2.75)$) and different values of the flow index ($n = (0.25, 1, 1.75)$).

Considering other values for Womersley and Weissenberg numbers we get the same solution behavior shown in Figure 3 for different values of flow index.

## IV. PERTURBED FLOWS

It is important to determine the changes in flow characteristics induced by perturbations in the initial or boundary data, body forces or pressure drop. In fact, since it is virtually impossible to maintain an exactly constant pressure drop, one should be able to predict how much a perturbation of given magnitude in pressure drop will affect the volume flow rate. We will consider a uniform perturbation of magnitude $\varepsilon$. For each $\varepsilon > 0$, defining the quantities,

$$\hat{G}_\varepsilon^\pm(\hat{t}) = (1 \pm \varepsilon)\hat{G}(\hat{t}), \qquad (41)$$

we denote by $\hat{Q}_\varepsilon^+$ and $\hat{Q}_\varepsilon^-$ the perturbed volume flow rates corresponding to the perturbation quantities $\hat{G}_\varepsilon^+$ and $G_\varepsilon^-$, respectively.

### Flow under constant mean pressure gradient

Considering the perburbation

$$\hat{G}_\varepsilon^\pm = (1 \pm \varepsilon)\hat{G}_0,$$

where $\hat{G}_0$ is a constant mean pressure gradient, for sufficiently large $\hat{t}$, after the transient period, we can use the characterization of the steady solution deduced in (39), and explicitly compute the perturbed volume flow rates, using (41), as follows:

$$
\begin{aligned}
\hat{Q}_\varepsilon^\pm &= \frac{1}{4}\hat{G}_\varepsilon^\pm = \frac{1}{4}(1 \pm \varepsilon)\hat{G}_0 \\
&= \hat{Q}(1 \pm \varepsilon).
\end{aligned} \qquad (42)
$$

Normalizing the above perturbeded volume flow rate $\hat{Q}_\varepsilon^\pm$ by the unperturbed volume flow rate $\hat{Q}$, we get

$$\frac{\hat{Q}_\varepsilon^\pm}{\hat{Q}} = (1 \pm \varepsilon), \qquad (43)$$

which means that in the steady case, this kind of multiplicative perturbation acts linearly. Changing the mean pressure gradient by a factor of $(1 \pm \varepsilon)$ changes the unperturbed volume flow rate by a factor of $(1 \pm \varepsilon)$. In particular this shows that the steady state solution is linearly stable. Perturbations will be negligible if $(1 \pm \varepsilon) \simeq 1$, which happens when $\varepsilon \to 0$, i.e. for small changes in the pressure gradient.

### Flow under time dependent mean pressure gradient

In the case of time dependent mean pressure gradient the same ideas hold, apart from the fact that it is no longer possible to deduce exact expressions for the perturbed volume flow rate. However, we can compute the time evolution of the perburbation volume flow rate $\hat{Q}_\varepsilon^+$ and $\hat{Q}_\varepsilon^-$. In Figure 4 we represent the time evolution of
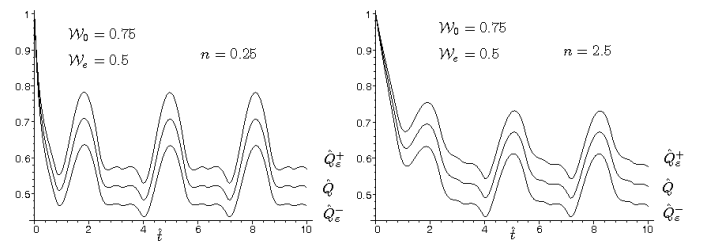


Fig. 4: Time evolution of the unperturbed volume flow rate $\hat{Q}$, and perturbeded volume flow rates $\hat{Q}_\varepsilon^\pm$, with $\mathcal{W}_e = 0.5$, $\mathcal{W}_0 = 0.75$ and flow index $n = (0.25, 2.5)$.

the volume flow rate using

$$\hat{G}(\hat{t}) = 1 + |\sin(\hat{t})| + |\cos(2\hat{t})| \qquad (44)$$

together with the perturbed flow rates of magnitude $\varepsilon = 0.1$, forming a strip around $\hat{Q}(\hat{t})$ containing all perturbations of magnitude less or equal to $\varepsilon$. Figure 5 shows
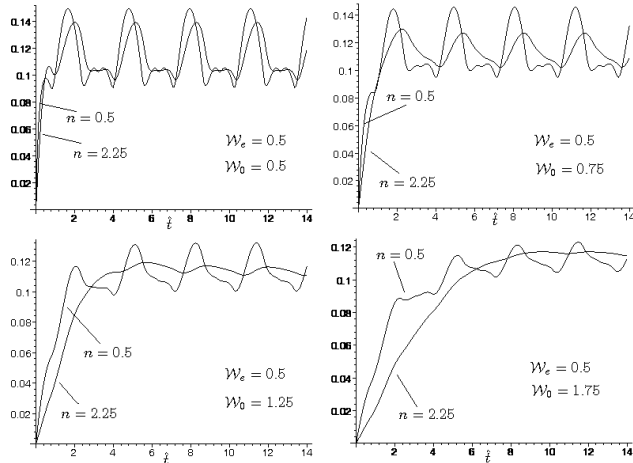
6

Fig. 5: Time evolution of perburbation (45) for different values of flow index $n$, with $\mathcal{W}_e = 0.5$ and $\mathcal{W}_0 = (0.5, 0.75, 1.25, 1.75)$.

the amplitude of this strip for several values of $n$, showing that increasing the flow index and the Womersley number reduces sensitivity to perturbations

$$|\hat{Q}_\varepsilon^+ - \hat{Q}_\varepsilon^-| \qquad (45)$$

with fixed Weissenberg number. Considering other values for Womersley and Weissenberg numbers we get the same solution behavior shown in Figure 5.

## V. CONCLUSIONS

A nine-director theory has been used to derive a 1D generalized second-order fluid model in a straight and rigid tube with circular cross-section and constant radius, as an alternative approach to predict some of the main properties of the associated 3D model $(10) - (13)$. Unsteady nondimensional relationship between mean pressure gradient and volume flow rate over a finite section of the tube has been obtained by introducing a shear-dependent function of power law related with the normal stress coefficients. In the case of unsteady/steady mean pressure gradient we predicted some numerical results for different values of flow index, Weissenberg and Womersley numbers. Finally, we conducted numerical simulations of perturbed flows, obtaining an exact expression for the perturbed volume flow rates in the steady case, providing a first step towards stability analysis of the model. Future work will be mainly directed to the application of this approach theory, related with the model $(10) - (13)$, for different geometries with the specific Carreau-Yasuda shear-dependent viscoelastic function.

## References

[1] J. Harris, Normal stress measurement in viscoelastic flow, *B. J. Appl. Phys.*, Vol.14, pp. 307-308, 1963.

[2] S.E. Mall-Gleissle, W. Gliessle, G.H. Mckinley, and H. Buggisch, The normal stress behavior of suspensions with viscoelastic matrix fluids, *Rheol.*, Vo.41, pp. 61-76, 2002.

[3] M. Beracea, C. Peati, B. Simionescu, and P. Navard, Shear rheology of semi-dilute poly-methyl-methacrylate solutions, *Macromolecules*, Vol.26, pp. 7095-7096, 1993.

[4] D.A. Caulk, and P.M. Naghdi, Axisymmetric motion of a viscous fluid inside a slender surface of revolution, *Journal of Applied Mechanics*, Vol.54, pp. 190-196, 1987.

[5] A.M. Robertson, and A. Sequeira, A Director Theory Approach for Modeling Blood Flow in the Arterial System: An Alternative to Classical 1D Models, *Mathematical Models & Methods in Applied Sciences*, 15, nr.6, pp. 871-906, 2005.

[6] F. Carapau, and A. Sequeira, 1D Models for blood flow in small vessels using the Cosserat theory, *WSEAS Transactions on Mathematics*, Issue 1, Vol.5, pp. 54-62, 2006.

[7] F. Carapau, and A. Sequeira, Axisymmetric motion of a second order viscous fluid in a circular straight tube under pressure gradients varying exponentially with time, *WIT Transactions on Engineering Sciences*, Vol.52, pp. 409-419, 2006.

[8] F. Carapau, A. Sequeira, and J. Janela, 1D simulations of second-grade fluids with shear-dependent viscosity, WSEAS Transactions on Mathematics, Issue 1, Volume 6, pp. 151-158, 2007.

[9] F. Carapau, and A. Sequeira, Unsteady flow of a generalized Oldroyd-B fluid using a director theory approach, *WSEAS Transactions on Fluid Mechanics*, Issue 2, Vol.1, pp. 167-174, 2006.

[10] F. Carapau, Numerical simulations of a second-order fluid with normal stress coefficients depending on the shear rate, *Proceedings of the American Conference on Applied Mathematics*, Harvard University, Cambridge, MA, USA, March 24-26, pp. 389-395, 2008.

[11] B.D. Coleman, and W. Noll, An approximation theorem for functionals with applications in continuum mechanics, *Arch. Rational Mech. Anal.*, Vol.6, pp. 355-370, 1960.

174

7

[12] R.S. Rivlin, and J.L. Ericksen, Stress-deformation relations for isotropic materials, *Journal of Rational Mech. Anal.*, Vol.4, pp. 323-425, 1955.

[13] J.E. Dunn, and R.L. Fosdick, Thermodynamics, stability and boundedness of fluids of complexity 2 and fluids of second grade, *Arch. Rational Mech. Anal.*, Vol.56, pp. 191-252, 1974.

[14] R.L. Fosdick, and K.R. Rajagopal, Anomalous features in the model of "second order fluids", *Arch. Rational Mech. Anal.*, Vol.70, pp. 145-152, 1979.

[15] V. Coscia, and G.P. Galdi, Existence, uniqueness and stability of regular steady motions of a second-grade fluid, *Int. J. Non-Linear Mechanics*, Vol.29, No.4, pp. 493-506, 1994.

[16] G. Tao, W.K. Otter, and W.J. Briels, Shear viscosities and normal stress difference in rigid liquid-crystalline polymers, *Macromolecules*, Vol.39, pp. 5939-5945, 2006.

[17] G.P. Galdi, A. Vaidya, M. Pokorný, D. Joseph, and J. Feng, Orientation of symmetric bodies falling in a second-order liquid at nonzero Reynolds number, *Mathematical Models and Methods in Applied Sciences*, Vol.12, No.11, pp. 1653-1690, 2002.

8